

Boosted Semantic Embedding based Discriminative Feature Generation for Texture Analysis

Priyadarshini K and Subhasis Chaudhuri

Abstract—Learning discriminative features is crucial for various robotic applications such as object detection and classification. In this paper, we present a general framework for the analysis of the discriminative properties of haptic signals. Our focus is on two crucial components of a robotic perception system: discriminative feature extraction and metric-based feature transformation to enhance the separability of haptic signals in the projected space. We propose a set of hand-crafted haptic features (generated only from acceleration data), which enables discrimination of real-world textures. Since the Euclidean space does not reflect the underlying pattern in the data, we propose to learn an appropriate transformation function to project the feature onto the new space and apply different pattern recognition algorithms for texture classification and discrimination tasks. Unlike other existing methods, we use a triplet-based method for improved discrimination in the embedded space. We further demonstrate how to build a haptic vocabulary by selecting a compact set of the most distinct and representative signals in the embedded space. The experimental results show that the proposed features augmented with learned embedding improves the performance of semantic discrimination tasks such as classification and clustering and outperforms the related state-of-the-art.

Index Terms—Haptic vocabulary design, boosted semantic embedding, distance metric learning, discriminative spectral feature, haptic textures.



1 INTRODUCTION

Understanding different sensory inputs is essential for designing autonomous robots and artificial intelligence (AI) devices. In order to perform real-world operations, a robot must be able to perceive, comprehend, and discriminate objects in its surroundings. While visual perception is sufficient for most robotics applications [1], [2], [3], some challenging real-world scenarios require additional sensory input such as tactile feedback to discriminate objects with similar visual features or to overcome vision limitations such as occlusion. In this work, we aim to develop a general framework for the analysis of the discriminative properties of haptic signals, specifically (a) what features enable *high automated discrimination* of different real-world signals, and (b) how we can effectively improve *semantic discrimination* of these signals by projecting signals in the embedding space using a learned distance metric. Our specific focus is on haptic textures: force feedback recordings of different surface materials, which can be played back via a haptic renderer. We use the texture database provided by Strese *et al.* [4]

Discriminative feature plays a crucial role in several applications such as object detection [1], semantic classification [4], [5], and scene understanding [3]. Some recent works [6], [7], [8] explore methods for surface material classification using multi-modal features. The method shows improvement in classification performance by combining haptic and visual features. However, in cases where only the haptic

modality (acceleration data) is used to generate features, the reported classification accuracy is low ($\sim 30\text{-}40\%$). Only with the inclusion of other modalities such as image, sound, friction, and scanning velocity does the accuracy improve. However, this requires additional sensing hardware, which adds cost and reduces the general-purpose usability of haptic devices. Moreover, the feature vectors in some of these works are also quite high-dimensional (e.g., 125-D in [9]), which can lead to overfitting. Further, none of the above methods show the significance of the distance metric in improving classification performance.

Learning an appropriate distance metric is fundamental to the robotic perception system. Several applications, including assistive devices such as digital screen reader, color identifiers, and navigational tools design, require a set of well distinguishable haptic signals for effective communication. Most often, in the original data representation, no underlying pattern is easily visible. The data is typically too high-dimensional, and different classes of signals are not well-separated in this space. To see the structural pattern within the data, we must project it to a (typically lower-dimensional) feature space through an appropriate transformation. Depending upon how the projection operator is learned, the projected data reflects the distinguishability between signals. We use a standard distance metric learning approach that projects feature to an embedding space such that similar materials are placed together and dissimilar ones far apart. Some prior works [10], [11] use the MDS-based projection approach. However, these methods are non-parametric and cannot compute a suitable projection of a new signal with new features at test time.

We propose a **general computational framework**,

• All authors are with IIT Bombay.
Email: priyadarshini.k@iitb.ac.in, sc@ee.iitb.ac.in

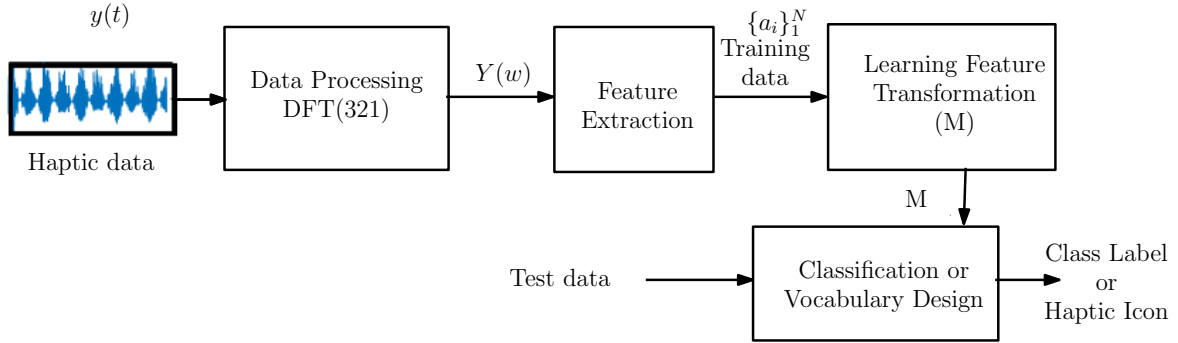


Fig. 1: Overview of the proposed algorithm.

founded on a novel set of **spectral features** for haptic textures generated only from acceleration data, augmented by a **boosted embedding** technique trained with semantic supervision. Such embedding has several important benefits. The performance of various pattern recognition algorithms, such as classification and clustering, can improve significantly after re-scaling the data using a learned embedding [12]. The embedding can also be used for evaluating the perceptual dissimilarity between two data points: first, the data are projected using a learned distance metric, and then a standard Euclidean metric is used to compute dissimilarity [13]. Some recent work in computer vision and image processing explores some of these ideas [14], [15]. However, this area is relatively unexplored in the haptics domain.

Contributions: The primary contributions of our work are as follows:

- 1) We propose a novel set of spectral features that enable discrimination of different real-world textures. We call this constant Q-factor filter bank (CQFB) feature, and it's briefly described in [13].
- 2) We present a general framework for the semantic discrimination of haptic signals. We demonstrate that the CQFB feature augmented with the boosted embedding gives much better performance of semantic discrimination tasks such as classification and clustering than without embedding.
- 3) Further, we demonstrate how to build a compact, discriminative dictionary of haptics signals by choosing a small, well-separated set of landmarks of the embedding space. In our knowledge, it is not done in any prior work. Our experimental results show that the discrimination error of the constructed vocabulary is significantly lesser than for any randomly chosen subset. An overview of our framework is shown in Fig. 1.

2 RELATED WORK

We overview two main areas of research relevant to our work: algorithms for surface material classification and strategies to construct a haptic vocabulary of most distinct signals.

2.1 Haptic Surface Classification

Distinguishing between surface materials using haptic touch is difficult due to the presence of high-frequency vibrations component in the texture signals. Several prior works use different discriminative textural features such as roughness, friction, and hardness of materials for classification tasks [4], [6], [8], [9], [16], [17], [18]. Strese *et al.* [4], [6], [8] use multi-modal feature (tactile and visual) to improve the performance of classifier. Authors in [6], [7] employ the powerful capability of the deep neural network to learn automated discriminative features, again using multi-modal sensory inputs. Joseph *et al.* [5] and Strese *et al.* [4] report very low classification accuracy ($\sim 30\text{-}40\%$) when haptic data (acceleration signal) alone is used for feature extraction. Joseph *et al.* [5] and Jeremy *et al.* [19] shows that successful recognition of surface material depends on scanning velocity and normal force applied during recording. Strese *et al.* [16] mitigates this effect by proposing a deep neural network approach that learns features from acceleration and tapping data.

Another exciting line of work [9], [19], [20] shows along with tactile information, the prior knowledge of exploratory movements is also needed to characterize the objects. A study by Lederman *et al.* [20] shows significant improvement in KNN classification accuracy (from 48% to 68%) using multiple exploratory movements. Further, Jeremy *et al.* [19] build an advanced model that adaptively selects the optimal feature and the optimal exploratory movements. Moreover, they use a high-end BioTac sensor for haptic data recording, which has similar mechanical properties as a human fingertip. They report a classification accuracy of around 95% on 117 textures. In contrast to our approach, all methods use either multi-modal or high-end data recording sensors such as a biomimetic sensor and multiple exploratory movements for feature generation. Our approach tries to classify 69 surface materials using the **acceleration data alone**, which is recorded using a low-cost acceleration sensor (LIS344ALH) in a **single exploration**. The dimension of our feature vector is also low (only 10-13). Moreover, our method provides a formal and general representation of haptic textures that directly captures the relationship between different signals in terms of similarity or dissimilarity.

2.2 Haptic Vocabulary Design

There are only a few papers that study methods to build a haptic vocabulary of representative haptic signals. Hollins *et al.* [10] proposed an embedding method that projects surface textures into lower dimensional space where Euclidean distance between surface textures reflects perceptual dissimilarity between them. The technique uses multidimensional scaling (MDS) for mapping inputs to lower-dimensional space. Enriquez *et al.* [11], who develop a set of 9 haptic icons that are perceptually well separated and distinguishable, again using MDS [21]. In contrast to these work, we use a parametric distance metric learning approach for modeling dissimilarity between haptic signals. Unlike the MDS-based approach, our approach learns the embedding as a function of signal features. It can be directly applied to compute a suitable projection of a new signal with new features, whereas MDS is a non-parametric mapping that does not extend to new unseen samples. Moreover, the MDS method is not easily adapted to different kinds of constraints.

3 METHOD

In this section, we present the various stages of our framework. First, we describe the initial data processing step and then explain how we construct our features and learn the embedding to improve separability between two materials in Section 3.1 and Section 3.2, respectively. Our objective is to learn a distance metric over the input space consisting of haptic data (acceleration data) of different surface materials such as stone, wood, grass, paper, etc. The learned distance metric re-scale the data in the embedding space such that the dissimilar haptic signals (say stone and grass) are placed far apart, and a similar pair (say stone and granite) are placed close together. Among the freely available dataset [4], [22], we choose texture datasets provided by [4] for our study. Unlike image or audio data, haptic data are not widely available. Although our method does not pose any limitation to use a specific kind of dataset, we choose this dataset because data recording is done in a controlled environment with respect to scanning force and speed. Hence the features are more reliable. The given dataset consists of acceleration signal, sound, friction force, and image of 69 different surface materials. The acceleration signal is recorded using an acceleration sensor attached with a haptic stylus. The detailed procedure of data recording is explained in [4].

To reduce the dimension of data, we combine the three components of the acceleration signal to one using DFT321 [23]. As mentioned in [23], the method preserves the spectral characteristic of the acceleration signal even after reducing the dimension. The psychophysical studies show that touch is highly sensitive up to 1 kHz frequency, and the optimal sensing frequency is around 250 Hz [24]. We thus have taken a signal spectrum within the frequency of 1 kHz for feature extraction. The various stages involved in our algorithm are illustrated in Fig. 1. Each stage of the algorithm is explained in the following sections.

3.1 Feature extraction

The major problem in learning discriminative feature with time series data is the phase invariant compact representation. Moreover, the distance metric used for feature transformation heavily relies on the meaningful feature to place similar data close to each other and dissimilar data far apart. However, in a high dimensional space, like in the case of time-series data, the contrast between similar and dissimilar data decreases [25]. In other words, the distance between two similar points almost approaches the distance between two dissimilar points. Moreover, high dimensionality in data makes the algorithm computationally expensive. Therefore it is essential to select the right feature set which can compactly represent the input data, keeping only important information while discarding the noise and redundant data. The frequency-domain analysis of texture signal is useful in terms of the reduction of correlated data or noise. Hence in our learning algorithm, we use spectral features.

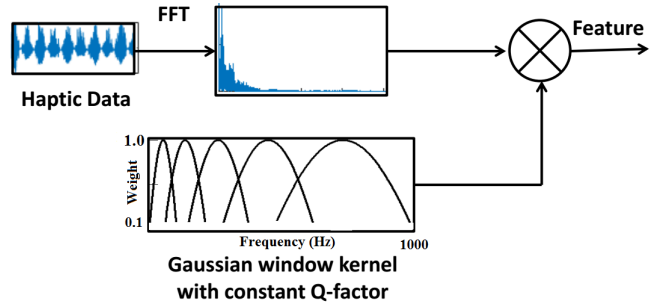


Fig. 2: Illustration of the feature extraction process. A variable bandwidth Gaussian shaped filter bank with constant Q-factor is used for feature extraction.

In [17], [19], [26], authors have either used low-frequency components of the signal or the k largest spectral coefficients as a feature vector. However, none of them can be used in our work. The signal of our interest (texture or vibration) is intrinsically high-frequency data. Therefore we cannot use just the low-frequency components of signal for feature extraction. Hence it is important to design a suitable feature space considering low as well as high-frequency components of the signal. We now describe the feature generation techniques that we have used. The proposed feature space was briefly introduced in [13] without any details. Note that our method only uses freehand movement acceleration data, unlike [4] and [16], where features are extracted using images, friction, sound, and acceleration data in the first case and tapping and movement acceleration data in the latter case.

We use DFT321 [23] to combine 3-axes acceleration data $y(t)$ into a single vector representing the spectral magnitude $Y(w)$. Subsequently, one can divide the entire spectrum into N number of bins of equal width, and compute the total spectral energy within each bin. This would leave us with a feature vector of length N . However, It has been shown that the human sensitivity to vibration is not a linear function of frequency; rather, it falls exponentially as frequency increases [27]. Hence a constant bandwidth bin would not serve the purpose of producing discriminative features. Hence we propose to vary the bin size in

geometric proportion as one moves from low frequency to high frequency, keeping the number of bins the same. Thus low-frequency components get more prominence compared to the high-frequency components, in addition to reducing the effect of noise in the data. Further, instead of using a rectangular window to integrate the spectral components within a bin, we use a window with an appropriate width of σ to provide certain spectral overlap between adjacent bins. We call these as constant Q factor filter-bank to obtain the feature vector. The process of feature extraction is illustrated in Fig. 2.

We apply a variable bandwidth Gaussian shaped filter bank $\{W_j(w)\}_{j=1}^N$ on frequency spectrum of the signal $Y(w)$ as shown in Fig. 2. The sigma(σ) and center frequency (f_c) of Gaussian kernel is varied in geometric progression with a constant Q factor α . At α equal to one, we get regularly spaced, constant bandwidth spectral bin. In order to keep the Q -factor constant, we vary the center frequency (f_c) as well as σ of the Gaussian kernel in geometric progression as follows-

$$f_{c_j} = \alpha^{j-1} f_{c_1}; \quad \sigma_j = \alpha^{j-1} \sigma_1; \quad j \in [1, N] \quad (1)$$

where N denotes the dimension of the feature vector. Since the central frequency of the last Gaussian window (f_{c_N}) cannot exceed the maximum frequency of spectrum (f_{max}), we have fixed f_{c_N} equal to f_{max} . Thereafter we compute other required parameters of the Gaussian filter bank as follow-

- 1) First we find center frequency of the first Gaussian window (f_{c_1}) using Eq. 1, ie, $f_{max} = \alpha^{N-1} f_{c_1}$.
- 2) Now we compute sigma of the first Gaussian window (σ_1) such that its passband dies down to 10% level at zero frequency, ie, $e^{-\frac{f_{c_1}^2}{2\sigma_1^2}} = 0.1$.

Having estimated f_{c_1} and σ_1 , one can find f_{c_j} and $\sigma_j \quad \forall \quad j$ using Eq.1. One may note that $\frac{f_{c_j}}{\sigma_j}$ is the same for all j and hence the Q factor is constant. The computed j^{th} component of feature is given by

$$a_j = \int_{f_{j-1}}^{f_j} W_j(w) |Y(w)|^2 dw \quad j \in [1, N] \quad (2)$$

We call the derived feature $x = \{a_1, a_2, \dots, a_N\}$ as constant Q -factor bandwidth (CQFB) feature. The next step of our algorithm is to learn an appropriate distance metric on the feature space for better distinguishability of haptic textures.

3.2 Learning semantic embedding

Our goal is to learn a feature transformation matrix $M \in \mathbb{R}^{N \times N}$ such that in the projected space, the Euclidean distance between two haptic signals is indicative of dissimilarity between them. We use the metric learning algorithm proposed by Chunhua *et al.* in [28] for feature transformation. Mahalanobis distance matrix is one of the popular distance metrics that define the distance between two points x_i and x_j as

$$d_M(x_i, x_j) = \|x_i - x_j\|_M = \|L(x_i - x_j)\|_2 = \sqrt{(x_i - x_j)^T M (x_i - x_j)} \quad (3)$$

where $M = L^T L$ is the learned $N \times N$ matrix and $x_i, x_j \in \mathbb{R}^N$. Estimating the Mahalanobis distance $d_M(x_i, x_j)$ is equivalent to first transforming the data into a new space by using projection $x \rightarrow L^T x$ and then applying Euclidean metric on the transformed data. When M is an identity matrix, the distance turns out to be Euclidean distance. One of the major challenges in learning the Mahalanobis matrix is to ensure the positive semi-definiteness constraint on the learned matrix M . To ensure positive semi-definiteness, sometimes transformation matrix L is learned instead of M [29], [30]. But this approach does not ensure the convergence to the global optimal value as the cost function becomes non-convex in this case. The standard SDP (semidefinite programming) solver can also be used to ensure the global optimum, but SDP is inefficient for metric learning, especially when the feature dimension is high. A different approach to circumvent the problem was proposed by Xing *et al.* in [12]. They use iteratively projected gradient descent method in which at each iteration, the solution is projected onto a positive semidefinite cone by decomposing the eigenvalues and substituting the negative eigenvalues by zero. The approach ensures the positive semi-definiteness of the matrix, but it offers a poor estimate of M .

3.2.1 Boosting technique

The BoostMetric technique [28] addresses this challenge by incorporating the properties of a positive semi-definite matrix in its learning approach itself. The technique is based on the properties that any positive semi-definite matrix can be decomposed into a linear combination of trace-one, rank-one matrices. Hence it tries to learn the trace-one and rank-one matrix iteratively. The final BoostMetric $M \in \mathbb{R}^{N \times N}$ takes form of $M = \sum_{k=1}^K w_k U_k$. The w_k is the non-negative weight and the matrix U_k is a trace-one, rank-one matrix. Apart from handling the positive-definiteness constraint elegantly, the BoostMetric has some additional desirable properties such as it is computationally less expensive, has the scalability to a large dataset, does not require parameter tuning like Adaboost [31] or LMNN [32]. Moreover, It fits very well to the domain of haptic texture discrimination, as it will be explained later.

The input to the boosting algorithm requires a set C of order relations among data.

$$C = \{(x_i, x_j, x_k) \mid d_M(x_i, x_j) < d_M(x_i, x_k)\} \quad (4)$$

Here the training samples x_i and x_j belong to the same class, and x_k belongs to a different class. The set of constraints C is in the form of triplets of training samples where the sample x_i is closer to sample x_j than x_k . The constraints are derived from the assumption that the distance among intra-class samples is smaller than inter-class samples. Hence in the framework of BoostMetric, we want to minimize the intra-class distance and maximize the inter-class distance. In order to create well separated clusters of different classes, we maximize the distance margin between the pair (i, j) and (i, k) . The expression for distance margin (ρ_r) of r^{th} triplet can be written mathematically as -

$$\rho_r = (x_i - x_k)^T M (x_i - x_k) - (x_i - x_j)^T M (x_i - x_j) \quad (5)$$

where $r \in \{1, 2, \dots, |C|\}$. $|C|$ is the cardinality of triplet set C defined in Eq. 4.

3.2.2 Optimization

As mentioned earlier, the aim is to maximize the distance margin (ρ_r) with an appropriate regularization. The optimization problem is defined [28] using an exponential loss function as follow

$$\begin{aligned} \underset{\mathbf{M}}{\text{minimize}} \quad & \log\left(\sum_{r=1}^{|\mathbf{C}|} \exp(-\rho_r)\right) + v\text{Tr}(\mathbf{M}) \\ \text{subject to} \quad & \mathbf{M} \succeq 0. \end{aligned} \quad (6)$$

Here v is a regularizing parameter. The regularizer term prevents the case where optimization problem leads to learning an arbitrarily large M to make the exponential loss zero. Note the in the boosting technique distance metric M is learned by incrementally adding the rank-one and trace-one matrices U_k as bases learners. The crucial part of solving the optimization problem 6 is estimating all basis learners $U_k (k = 1 \dots K)$ and the number of such possible U 's is infinite. Therefore, instead of directly solving the primal problem 6, the column generation technique [33] is used, which finds the approximate solution by estimating the subset of entire variables set at each step. The new variable is learned incrementally only if it improves the solution significantly. The details of the algorithm can be found in [28].

4 EXPERIMENTS

We conduct various experiments to evaluate the accuracy and effectiveness of our algorithm. Firstly, we demonstrate how the defined CQFB feature and the learned embedding improve the performance of texture classification tasks. Then we show how to construct a dictionary of distinct domain signals in the embedding space. In each case, we compare the performance to those alternatives from ablation studies or prior work. To ensure the comparability of different methods, the same test data is used for all tested methods. Our implementations are in Matlab, and we used the reference code from authors' websites as appropriate. Our data are drawn from the TUM texture repository [4]. The dataset has acceleration data corresponding to 69 different surface materials. The recording of training and testing data is done separately by different users. The training data is recorded by domain experts, whereas testing data is recorded by subjects unfamiliar with work details. Each training and testing data contains 690 samples, ten samples in each class. In the prior work [4], the algorithm is evaluated using 69 different surface materials. The detail of the data recording procedure is described in [4]. We treat the samples within a class as equivalent, and randomly pick a representative every time we need features for a class. For all experiments below, testing is done on a separately recorded testing dataset, which is different from the training dataset.

4.1 Classification results

In this section, we show the discriminative power of the proposed boosted semantic embedding of haptic signals. Training signals are labeled by their class, and BoostMetric training triplets are constructed with two samples from a single class and the third sample from a different one. We seek to show that classes of signals are easily separable in

Feature	Accuracy(%)	Accuracy(%)	Reference
	Without BM	With BM	
Spectral Peak	12	12	[26]
Spectral frequency	2	4	[26]
Energy Values	43	65	[5]
CQFB($\alpha = 1$)	2.5	13	Sec. 3
CQFB($\alpha = 1.8$)	60	82	Sec. 3

TABLE 1: Comparison of k -NN classification performance with different features. The results show the improvement in classification accuracy for different features when the BoostMetric(BM) is used in conjunction.

the embedding space and hence perform a better classification task: predicting which of the 69 classes an unlabeled test signal belongs to. From a total of 690 training samples, we generated a total of 6210 triplets and trained BoostMetric M with a regularizing parameter $v = 10^{-7}$ in Eq. 6, for 3000 iterations.

Our work rests on two key contributions: (a) the CQFB(Constant Q-factor bandwidth) features that capture salient features of the acceleration data, and (b) the BoostMetric-based feature transform that further enhances separability of signals in the projected space. To demonstrate the individual role of each of these factors to the overall efficacy of the method, we conduct various ablation studies in which we choose different features, or omit the metric embedding, or both. The results for the classification of unseen test signals with different features are given in Table 1. In the first experimentation, Our boosted features use only a simple k -NN ($k = 3$) classifier, to highlight the advantages of the features alone. The classification performance of various other classifiers is presented later in the section.

Table 1 shows the comparison of k -NN classification performance with different features from prior work, in original feature space, and in the learned boosted embedding space. Experimentation is done for various feature dimension, and the best accuracy is reported for each feature in the Table 1. As we can see, some of the features such as spectral peak, spectral frequency cannot capture the hidden features of the data well. Note that the CQFB feature with constant bandwidth ($\alpha = 1$) also fails to capture the complexity of underlying data. This is expected, as the discriminating power is better at a lower frequency, and by using an equal bandwidth filter, we lose signal feature by capturing lower frequency components at a low resolution. Using a variable bandwidth CQFB feature, accuracy improves significantly (from 2.5% to 60%). This further validates the significance of using CQFB feature in the classification task. As we can see from Table 1, BoostMetric consistently improves k -NN classification accuracy for most of the features, and the best accuracy is achieved with the combination of the CQFB feature and boosted embedding.

For comparison, we also present accuracies with a variety of other features and classification methods from prior work. Table 2 reports various other classifier's results and its comparison from related work by Strese *et al.* [4]. In [4], authors present the classification results of Naive Bayes classifier and Decision Tree with several features. Note that all unimodal features which are obtained from acceleration data alone have low accuracy ($\leq 39\%$), and the accuracy

Feature	Data Type	Dimension	Naive Bayes (%)	Decision Tree (%)	Reference
LPC Coefficients	Acc	10	5	4	[4], [17]
Spectral Peaks	Acc	5	9	9	[4], [26]
Standard Roughness	Acc	1	11	10	[4], [19]
Energy Values	Acc	30	29	30	[4], [5]
Spectrogram	Acc	125	39	29	[4], [9]
AIH, AMTR, SIH	Acc, Img				
ICOA, IG, FM	Snd, Frc	6	74	67	[4]
CQFB($\alpha = 1.8$)	Acc	11	72	69	Our method

TABLE 2: Comparison of classification performance of our approach and related work by Strese *et al.* [4]. The results of related work is taken from the corresponding paper [4]. Some abbreviation used are as follows: Acc (acceleration), Img (Image), Snd (sound), Frc (friction), CQFB(Constant Q-factor filter bank), AMTR (Acceleration movement temporal roughness), SIH (Sound Impact Hardness), IG (Image Glossiness), FM (friction feature), AIH (acceleration impact hardness), ICOA (Image coarseness of average gray level).

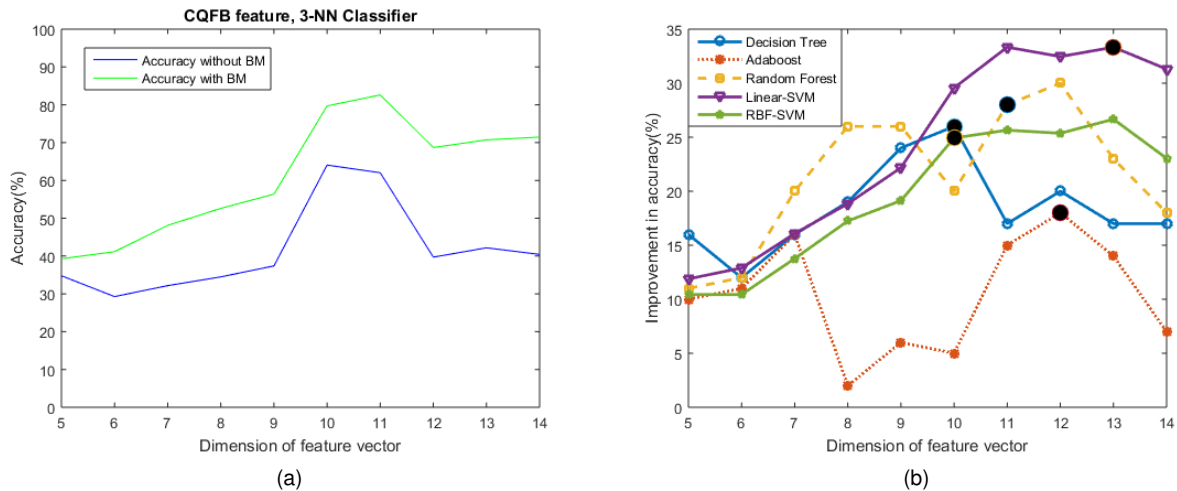


Fig. 3: Performance of K-NN classifier in Euclidean and boosted embedding space as a function of the CQFB feature dimension. The second figure shows the increment in the classification accuracy in embedded space over Euclidean space for different classifiers. The black circle in each incremental curve denotes the dimension at which we obtained the best classification result. The best accuracy attained by different classifiers are as follow - Decision tree (72% at feature dimension 10), Adaboost (54%, dimension 12), Random Forest classifier (86%, dimension 11), Linear SVM (78%, dimension 13), RBF kernel SVM (70%, dimension 10).

improves to 74% for Naive Bayes classifier and 67% for Decision Tree only when other modalities of data are used for features extraction. In contrast, CQFB feature augmented by boosted embedding technique yields promising results only with acceleration data and is beaten marginally only by the method that resorts to other modalities to improve recognition.

Further, we compare in Fig. 3 the performance of learned distance metric with the baseline Euclidean distance metric for classification task across various features dimensions using the CQFB feature. It can be observed that by use of BoostMetric improves the accuracy of the KNN classifier significantly. In Fig. 3b we study the same for other types of classifiers that one may select. As we can see in Fig. 3b, the classification performance of all classifiers improves in the embedding space. This validates that the learned distance metric is much more effective in improving the separability of data than the Euclidean metric.

We visualize the embedding space (projected to 2D using t-SNE [34]) in Figure 4, with just randomly chosen ten classes out of 69 for clarity. On the left (a), we see

constant bandwidth CQFB features ($\alpha = 1$) fail to recover the underlying data structure. In the middle (b), variable bandwidth CQFB features form clear class-based clusters, but they are fairly diffused, and it is easy to see how a simple classifier can confuse similar classes near their class boundaries. On the right (c), BoostMetric induces more compact clusters with low intra-class variance, but high inter-class separation. Classes are much better separable in Fig. 4c.

4.2 Haptic texture discrimination

In this section we evaluate the performance of learned embedding in discriminating surface materials using acceleration data. We measure discriminability of two surface materials as the average number of triplet (x_i, x_j, x_k) comparisons which satisfies the constraints $(d_M(x_i, x_j) < d_M(x_i, x_k))$. We define dissimilarity index p_{bc} for each material pair (b, c) as follow:

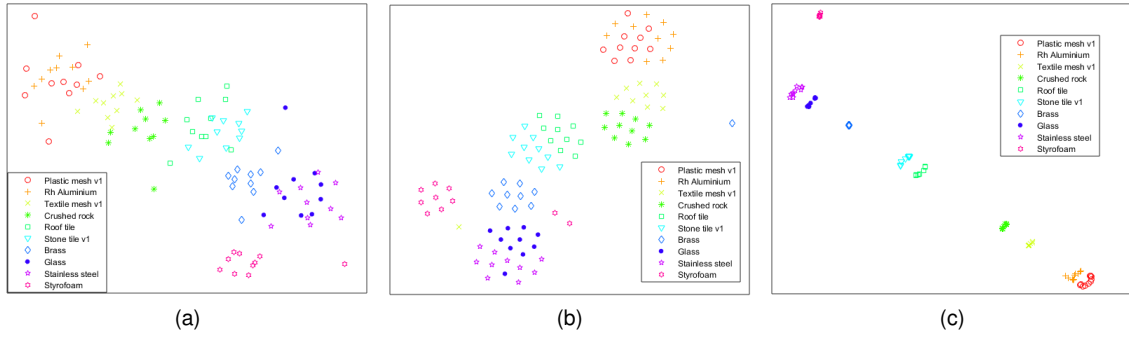


Fig. 4: Illustrating improved separability of classes due to the choice of CQFB feature and BoostMetric embedding. Different symbols and colors indicate different materials. Features are projected onto 2D space using t-SNE plot, (a) Constant bandwidth feature (CQFB features with $\alpha = 1$), (b) Variable bandwidth feature (CQFB features with $\alpha = 1.8$) and (c) Variable bandwidth feature (CQFB features with $\alpha = 1.8$) projected after embedding.

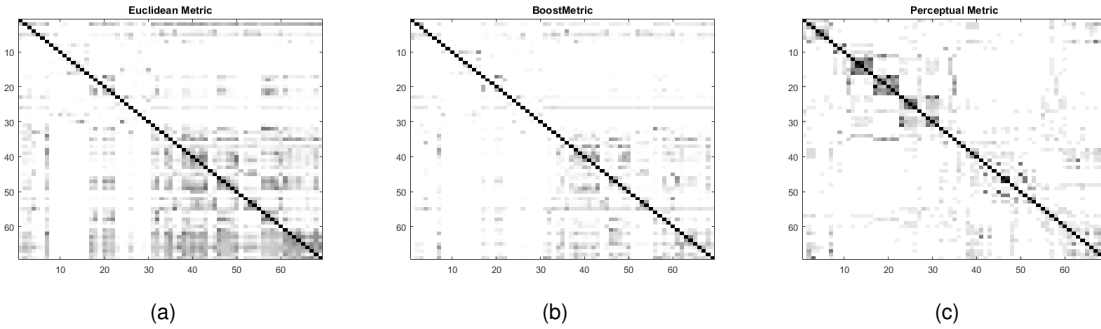


Fig. 5: Confusion matrix (69×69 matrix) while discriminating different texture pairs obtained with (a) Euclidean metric, (b) BoostMetric, and (c) Perceptual ground truth obtained from human perceptual judgment as provided in [4]. Darker spots indicate more confusion in distinguishing a pair of textures. The matrix shows many indistinguishable textures pairs in the Euclidean space. BoostMetric improves the separability of surface textures and surpasses even human distinguishing capability. Many texture pairs (such as brick (index = 8) and granite (index = 10)) that are difficult to discriminate by touch are readily distinguishable by BoostMetric, while some texture pairs (plastic mesh (index = 4) and carpet (index = 36)) that are easy to discriminate by a human were more challenging for BoostMetric.

$$p_{bc} = \frac{|S|}{|C_{bc}|}; S = \{(x_i, x_j, x_k) | d_M(x_i, x_j) < d_M(x_i, x_k)\} \quad (7)$$

where (x_i, x_j, x_k) is a triplet constructed from two signals x_i and x_j of same class b , and x_k from different class c and C_{bc} is a set of all possible triplets constructed from signals of class b and c without any constraint on the distance. The distance $d_M(x_i, x_j)$ is measured using equation 3. The dissimilarity index (p_{bc}) is a measure of the probability of distinguishing two materials in the embedded space using the learned distance matrix M . A small value of the dissimilarity index indicates a more confusing material-pair. Figure 5 shows the confusion matrix obtained using our model with CQFB features and employing the proposed embedding technique. The darker spots in the confusion matrix indicate more confusion in distinguishing texture-pairs. As we can see, materials are better separable in the embedded space than in the Euclidean space. The overall discrimination error is obtained by finding the mean of the confusion index of all material pairs. The average discrimination error in separating a material-pair using Euclidean

metric and BoostMetric are 7.10% and 3.76%, respectively, substantiating the usefulness of BoostMetric embedding. To quantitatively compare similarities between the estimated confusion matrices and the ground-truth confusion matrix (which is an identity matrix), we use RV-coefficient [35], [36]. The RV-coefficient is the two dimensional extension of Pearson correlation coefficient and it measures the similarity between two spatial patterns (say, square matrices S_1 and S_2). The coefficient takes a value between zero and one with a value close to one indicating a high degree of similarity between two patterns. If θ defines the correlation angle, it is given as

$$\theta = \arccos RV(S_1, S_2) = \arccos \left(\frac{\text{tr}(S_1^T S_2)}{\sqrt{\text{tr}(S_1^T S_1)} \sqrt{\text{tr}(S_2^T S_2)}} \right) \quad (8)$$

and for a good similarity with the ground truth the angle θ should be close to zero. The corresponding computed values of correlation angle θ from Fig. 5 are (i) 8.3° for Euclidean metric, (ii) 5.2° for the Boost metric and (iii) 5.4° for the human perception. This shows that the proposed

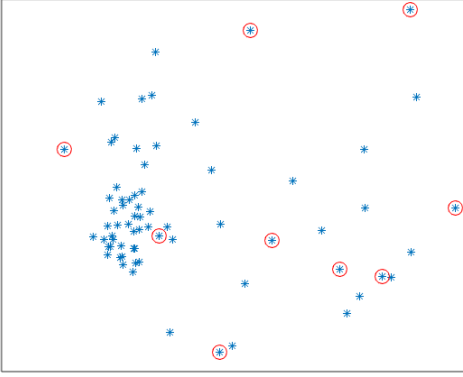


Fig. 6: Visualization of 69 haptic textures represented by class centroid (cluster center of CQFB features) projected on 2D space using MDS (multidimensional scaling). The red circles show nine most distant class centroid chosen out of 69 classes using the farthest point sampling method.

boost metric performs better than the Euclidean metric and is relatively closer to the human perception.

Further, we evaluate our model by comparing its performance with actual human subject performance in discriminating haptic textures. For human perceptual similarity feedback, we have used the similarity matrix \mathbf{S}_H provided by authors in [4]. Each element $\mathbf{S}_H(i, j)$ denotes the number of subjects (out of 30) having perceived different materials i and j to be similar and clubbed them into the same group. In other words, each element in the matrix \mathbf{S}_H indicates the confusion in separating two materials apart. We compute the average error made by a person in distinguishing a pair of materials to be 3.22% from [4]. However, the combination of the CQFB feature and our embedding technique yields 3.76% which is very close to human error. This shows that the proposed technique mimics human subject behavior closely. It may be noted that none of the methods, including the proposed one, considers the human perceptual limitation in its measure. Human perception is limited by the JND (just noticeable difference), while the computational methods leave no room for the incorporation of JND in the learned metric. The inclusion of human perceptual limitations in terms of JND in the distance metric learning process will definitely increase its usability. Next, we demonstrate the suitability of our approach in designing a vocabulary of most distinct haptic textures utilizing their representation in the embedded space.

4.3 Haptic Vocabulary Design

Given a signal set $X = \{x_1, x_2, x_3, \dots, x_m\}$, we need to choose a subset S of k signals which are farthest apart from each other. Thus out of possible m haptic icons, we need to select k of them to build a vocabulary so that this subset of icons has better discriminability among themselves. Generally, choosing such a subset S is an NP-hard problem, and it requires the knowledge of how to compute the mutual distances. One can approximate this combinatorially difficult subset selection problem by greedy algorithms such as farthest point sampling method [37]. In the farthest point sampling method, an initial point is chosen randomly, and

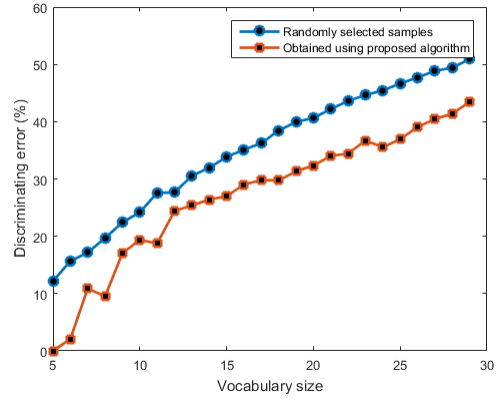


Fig. 7: Comparison of discrimination error for different vocabulary subset constructed using the proposed method and for randomly selected subset.

the farthest candidate point in the signal set X is selected iteratively. In each iteration, the algorithm selects the point which maximizes the minimum distance from the elements of the subset.

In order to build a vocabulary from the given texture dataset, we need to have a representative signal for each class. One may choose any random signal from the class or class centroid as a class representative. The class centroid is the cluster center of CQFB features for the available ten acceleration signals of given surface material. In this study, we represent each class by the class centroid as it better depicts the distribution of signals in the class as compared to any randomly chosen signal. However, the class centroid may not be the true representation of the class in the presence of outliers or if the class variance is high. To circumvent such issues, high-variance classes may be removed before selecting a set of most distinct signals using furthest point sampling. The method requires solving the following optimization problem for each candidate signal x_i until $|S| = k$.

$$\max_{S \subset X} \left(\min_{\substack{i \neq l \\ x_i \in S \\ x_l \in X \setminus S}} d_M(x_i, x_l) \right) \quad (9)$$

Iteratively, we add one sample from set X into set S and compute pairwise distances of all points in S to the points in X . The point with the maximum, minimum distance is selected and added into set S . Although the furthest point sampling approach works well with our dataset, it is quite inefficient for a larger dataset because, in every iteration, it requires the computation of distances among all pairs of samples. However, given the fact that the vocabulary has to be designed only once, it does not pose any undue burden. The algorithm is a greedy one; the set of selected points also depends on the initial points chosen. In our case, the initially chosen points are the most distant sample pair from set X .

To evaluate the effectiveness of our vocabulary, we compare the discrimination error of built vocabulary and the randomly selected subset of the same size. We compute the discrimination error using the eq. 7. Further, to evaluate the robustness of our method across different vocabulary sizes,

we construct a vocabulary of different sizes and compare its discriminability again with the randomly selected subset. Fig 7 shows the average discrimination error for the selected subset using our method is significantly lesser than the randomly selected subset across different vocabulary sizes.

5 CONCLUSIONS

In this work, we have presented a framework for the discriminative analysis of haptic textures using a learned distance metric. We have proposed a new set of hand-crafted features to represent haptic textures, which enable us to discriminate real-world surface textures. Further, we learned semantic embedding on the feature space using class-based supervision to improve separability between haptic signals. We found that our method outperforms the state-of-the-art method by a large margin in classification tasks when only the single-exploration acceleration data is used. The extensive experimentation shows how embedding in feature space improves the classification, clustering, and texture discrimination performances. Further, we demonstrate how to build a vocabulary of haptic signals that could potentially be used for haptic communication. Currently, our work does not take into account human perceptual limitations. Our future work will include this important aspect of capturing JND (just noticeable difference) of human subjects while computing the distance metric.

REFERENCES

- [1] E. Martinez-Martin and A. P. Del Pobil, "Object detection and recognition for assistive robots: Experimentation and implementation," *IEEE Robotics & Automation Magazine*, 2017.
- [2] S. Gu, E. Holly, T. Lillicrap, and S. Levine, "Deep reinforcement learning for robotic manipulation with asynchronous off-policy updates," in *2017 IEEE international conference on robotics and automation (ICRA)*. IEEE, 2017.
- [3] A. Nguyen, "Scene understanding for autonomous manipulation with deep learning," *arXiv preprint arXiv:1903.09761*, 2019.
- [4] M. Strese, C. Schuwerk, A. Iepure, and E. Steinbach, "Multimodal feature-based surface material classification," *IEEE transactions on haptics*, 2017.
- [5] J. M. Romano and K. J. Kuchenbecker, "Methods for robotic tool-mediated haptic surface recognition," in *Haptics Symposium (HAPTICS), 2014 IEEE*, 2014.
- [6] Y. Gao, L. A. Hendricks, K. J. Kuchenbecker, and T. Darrell, "Deep learning for tactile understanding from visual and haptic data," in *2016 IEEE International Conference on Robotics and Automation (ICRA)*. IEEE, 2016.
- [7] H. Zheng, L. Fang, M. Ji, M. Strese, Y. Özer, and E. Steinbach, "Deep learning for surface material classification using haptic and visual information," *IEEE Transactions on Multimedia*, 2016.
- [8] M. Strese, L. Brudermueller, J. Kirsch, and E. Steinbach, "Haptic material analysis and classification inspired by human exploratory procedures," *IEEE transactions on haptics*, 2019.
- [9] J. Sinapov, V. Sukhoy, R. Sahai, and A. Stoytchev, "Vibrotactile recognition and categorization of surfaces by a humanoid robot," *IEEE Transactions on Robotics*, 2011.
- [10] M. Hollins, R. Faldowski, S. Rao, and F. Young, "Perceptual dimensions of tactile surface texture: A multidimensional scaling analysis," *Perception & psychophysics*, 1993.
- [11] M. Enriquez, K. MacLean, and C. Chita, "Haptic phonemes: basic building blocks of haptic communication," in *Proceedings of the 8th international conference on Multimodal interfaces*, 2006.
- [12] E. P. Xing, M. I. Jordan, S. J. Russell, and A. Y. Ng, "Distance metric learning with application to clustering with side-information," in *Advances in neural information processing systems*, 2003.
- [13] K. Priyadarshini, S. Chaudhuri, and S. Chaudhuri, "Perceptnet: Learning perceptual similarity of haptic textures in presence of unordered triplets," in *IEEE World Haptics Conference (WHC)*, 2019.
- [14] T. Mensink, J. Verbeek, F. Perronnin, and G. Csorka, "Distance-based image classification: Generalizing to new classes at near-zero cost," *IEEE transactions on pattern analysis and machine intelligence*, 2013.
- [15] S. Liao, Y. Hu, X. Zhu, and S. Z. Li, "Person re-identification by local maximal occurrence representation and metric learning," in *Proceedings of the IEEE conference on computer vision and pattern recognition*, 2015.
- [16] M. Strese, C. Schuwerk, and E. Steinbach, "Surface classification using acceleration signals recorded during human freehand movement," in *IEEE World Haptics Conference (WHC)*. IEEE, 2015.
- [17] H. Culbertson, J. Unwin, and K. J. Kuchenbecker, "Modeling and rendering realistic textures from unconstrained tool-surface interactions," *IEEE transactions on haptics*, 2014.
- [18] B. A. Richardson and K. J. Kuchenbecker, "Improving haptic adjective recognition with unsupervised feature learning," in *2019 International Conference on Robotics and Automation (ICRA)*, 2019.
- [19] J. A. Fishel and G. E. Loeb, "Bayesian exploration for intelligent identification of textures," *Frontiers in neurorobotics*, 2012.
- [20] S. J. Lederman and R. L. Klatzky, "Haptic classification of common objects: Knowledge-driven exploration," *Cognitive psychology*, 1990.
- [21] K. MacLean and M. Enriquez, "Perceptual design of haptic icons," in *Proc. of EuroHaptics*, 2003, pp. 351–363.
- [22] H. Culbertson, J. J. Lopez Delgado, and K. J. Kuchenbecker, "The penn haptic texture toolkit for modeling, rendering, and evaluating haptic virtual textures," *Departmental Papers*, 2014.
- [23] N. Landin, J. M. Romano, W. McMahan, and K. J. Kuchenbecker, "Dimensional reduction of high-frequency accelerations for haptic rendering," in *International Conference on Human Haptic Sensing and Touch Enabled Computer Applications*, 2010.
- [24] L. Skedung, M. Arvidsson, J. Y. Chung, C. M. Stafford, B. Berglund, and M. W. Rutland, "Feeling small: exploring the tactile perception limits," *Scientific reports, Nature*, 2013.
- [25] K. Beyer, J. Goldstein, R. Ramakrishnan, and U. Shaft, "When is "nearest neighbor" meaningful?" in *International conference on database theory*, 1999.
- [26] N. Jamali and C. Sammut, "Majority voting: Material classification by tactile sensing using surface texture," *IEEE Transactions on Robotics*, 2011.
- [27] S. Bensmaïa and M. Hollins, "Pacian representations of fine surface texture," *Perception & psychophysics*, 2005.
- [28] C. Shen, J. Kim, L. Wang, and A. Hengel, "Positive semidefinite metric learning with boosting," in *Advances in neural information processing systems*, 2009.
- [29] J. Goldberger, G. E. Hinton, S. T. Roweis, and R. R. Salakhutdinov, "Neighbourhood components analysis," in *Advances in neural information processing systems*, 2005.
- [30] L. Torresani and K.-c. Lee, "Large margin component analysis," in *Advances in neural information processing systems*, 2007.
- [31] R. E. Schapire, "Theoretical views of boosting," in *European conference on computational learning theory*, 1999.
- [32] K. Q. Weinberger and L. K. Saul, "Distance metric learning for large margin nearest neighbor classification," *Journal of Machine Learning Research*, 2009.
- [33] A. Demiriz, K. P. Bennett, and J. Shawe-Taylor, "Linear programming boosting via column generation," *Machine Learning*, 2002.
- [34] L. v. d. Maaten and G. Hinton, "Visualizing data using t-sne," *Journal of machine learning research*, 2008.
- [35] P. Robert and Y. Escoufier, "A unifying tool for linear multivariate statistical methods: the rv-coefficient," *Applied Statistics*, 1976.
- [36] F. Kherif, J.-B. Poline, S. Mériaux, H. Benali, G. Flandin, and M. Brett, "Group analysis in functional neuroimaging: selecting subjects using similarity measures," *NeuroImage*, 2003.
- [37] T. Schlömer, D. Heck, and O. Deussen, "Farthest-point optimized point sets with maximized minimum distance," in *Proceedings of the ACM SIGGRAPH Symposium on High Performance Graphics*, 2011.